Physica C 179 (1991) 303–310
North-Holland

PHYSICA C

Interstitial doping and oxygen exchange in superconducting $La_2CuO_{4+\delta}$

N.D. Shinn, M.E. Bartram, J.E. Schirber, J.W. Rogers Jr. and D.L. Overmyer
Sandia National Laboratories, Albuquerque, NM 87185, USA

Z. Fisk and S.-W. Cheong
Los Alamos National Laboratory, Los Alamos, NM 87545, USA

Received 19 March 1991
Revised manuscript received 10 June 1991

The oxygen doping of lanthanum cuprate to generate superconductiving $La_2CuO_{4+\delta}$ ($0<\delta\leqq 0.032$) has been studied by high-pressure, isotopic-oxygen enrichment and thermal desorption mass spectroscopy (TDMS). Isotopic data show that the additional oxygen incorporated under high pressure readily exchanges with ionic lattice oxygen during enrichment at 860 K. The thermal release of the excess oxygen from superconducting crystals above ~350 K is not bulk diffusion limited. An alternate explanation for the observed rapid $O_2(g)$ bursts is proposed.

1. Introduction

La_2CuO_4 is the simplest layered cuprate compound which may be either substitutionally doped [$La_{2-x}(Sr, Ba)_xCuO_4$, $x\leqq 0.2$] or (uniquely) interstitially doped with oxygen [$La_2CuO_{4+\delta}$, $\delta\leqq 0.05$] to yield a superconducting phase with $T_c = 35$–40 K [1–3]. These doped compounds exhibit much of the interesting physics generic to hole-doped superconductors without the disadvantages of the more complex materials chemistry of the higher critical temperature materials. Perhaps the simplest of these materials is the reversibly doped, oxygen-enriched superconductor $La_2CuO_{4.032}$; the interstitial oxygen incorporated by high-pressure enrichment is readily released by annealing above ~350 K in air or vacuum to regenerate $La_2CuO_{4.00}$ [4,5]. This paper reports kinetic studies addressing the incorporation and release of this excess oxygen.

Early studies of *ceramic* $La_2CuO_{4+\delta}$ ($\delta\approx 0.13$) discovered that the excess oxygen incorporated by high-pressure annealing is evolved from the superconducting crystals in numerous, rapid bursts [5] of $O_2(g)$ when heated in vacuum above 400 K. Single-phase crystal studies [6] have established that the superconductor has an oxygen stoichiometry of $La_2CuO_{4.030\pm 0.005}$, illustrating that the high surface area ceramic samples retain oxygen extrinsic to the interstitially-doped bulk superconducting phase [7]. Correspondingly, fewer oxygen bursts are observed from single crystals when heated in ultra-high vacuum and continuous oxygen evolution is not observed if the crystal is held at a constant temperature.

Although the exact nature of the excess oxygen species remains controversial, powder neutron and X-ray diffraction data have been interpreted in terms of models with interstitial oxygen atoms [8,9]. These structural studies [10,11] have shown that $La_2CuO_{4+\delta}$ undergoes a tetragonal to orthorhombic phase transition below ~420 K. Below ~320 K, a further phase separation occurs [12] into a nonsuperconducting orthorhombic Cmca phase of essentially stoichiometric $La_2CuO_{4.00}$ and a second superconducting oxygen-rich phase of $La_2CuO_{4.048}$. These transition temperatures and the volume fractions of the two orthorhombic phases are dependent upon the initial interstitial oxygen concentration (δ) from each specific oxygen enrichment treatment. Single crystals annealed at 860 K and 3 kbar oxygen pressure for the present studies exhibit the tetrago-

0921-4534/91/$03.50

nal-to-orthorhombic transition at ~280 K and the orthorhombic phase separation at ~260 K [10,12]. This phase separation phenomenon supports the conclusion that the superconductivity results from the interstitial oxygen doping and not from oxygen or lanthanum lattice vacancies.

In the present work, isotopic oxygen enrichment and thermal desorption mass spectroscopy (TDMS) have been used to study dissociation, diffusion, and desorption of the interstitial oxygen central to these structural models. The measured kinetics of interstitial oxygen desorption from $La_2CuO_{4+\delta}$ are inconsistent with conventional first-order or second-order processes typically observed in thermal desorption from solid surfaces [13,14], demonstrating that neither bulk diffusion nor associative desorption are rate limiting steps. Instead, we propose an explanation involving internal lattice stresses leading to fracture, thereby liberating the excess oxygen in rapid bursts. We note that stress-induced crystal fracture is not uncommon for crystalline phase transformations that involve lattice expansions and concentrations [15], and could be exacerbated by mobile interstitial oxygen in $La_2CuO_{4+\delta}$.

2. Experimental procedures

Single crystal samples for the present experiments were grown and prepared following the same procedures used for the samples used in the diffraction studies reported earlier [6]. Crystals of $La_2CuO_{4.00}$ were grown at Los Alamos National Laboratory from a CuO-rich La_2O_3–CuO melt in a platinum crucible [2]. After quenching from high temperature, the insulating samples were oxygen-enriched at Sandia to superconductors by annealing in 1–3 kbar $^{16}O_2(g)$ (or 98% pure $^{18}O_2$) at 860 K for 12–100 h. The isotopically labeled oxygen was recovered after the high-pressure anneal and verified by mass spectroscopy to be $(98.4 \pm 0.4)\%$ $^{18}O_2(g)$. RF impedence measurements following oxygen enrichment verified a superconducting critical temperature between 35 and 40 K for each crystal. These irregularly-shaped crystals, like all macroscopic crystals, contain grain boundaries and internal defects which lead to a mosaic structure of well-oriented micro-single-crystallites. The crystals transform from tetragonal to orthorhombic structures upon cooling and usually consist of an intimate mixture of the two twins in which the *a* and *b* axes are interchanged. X-ray diffraction studies on these samples exhibit sharp diffraction peaks [6], demonstrating that the characteristic domain dimension within such twins exceeds ~2000 Å.

Individual crystals were weighed both before and after each oxygen enrichment treatment. The addition of 0.032 oxygen atoms to the parent 2-1-4 formula unit adds 0.12% and 0.13% to the molar mass for ^{16}O and ^{18}O, respectively, which are near the detection limits of a reliable weight determination. The irregularly shaped crystals were wrapped in a four-turn coil of 0.010 inch diameter molybdenum wire which served to hold a chromel/alumel thermocouple junction in contact with the crystal. This assembly was hung from a manipulator approximately 6 inches from the ionizer of a UTI 100C quadrupole mass spectrometer in a turbomolecular pumped, high-vacuum chamber. Because the TDMS $O_2(g)$ signal was unaffected by the background water partial pressure, a longer pump-down time at room temperature was substituted for a bake-out to avoid the possibility of inadvertently desorbing some of the interstitial oxygen during the bake-out.

For the TDMS experiments, the Mo wire surrounding the sample was resistively heated by a programmable power supply. The temperature ramp was linearized to less than 1 K s^{-1} at the heating coil using the thermocouple emf in a feedback circuit. While the temperature ramp was applied, the mass spectrometer repeatedly sampled up to nine mass channels with independently specified amplifier gains in a cycle time of ~200 ms. This procedure permitted redundant mass sampling and ensured that a suitable gain was selected to detect each mass of interest. The amplified analog mass spectrometer output (1–5 nA) at each sampling point was digitized and stored. Despite the slow heating rate, a significant temperature gradient across the sample was unavoidable, especially at high temperatures. After the TDMS experiments, a second thermocouple junction was embedded in a hole drilled in one $La_2CuO_{4.00}$ crystal away from the heater coils and used to calibrate the first thermocouple junction held by the heater coil.

3. Results

3.1. Oxygen desorption

Typical mass 32 desorption data for an insulating $La_2CuO_{4.00}$ sample and an $^{16}O_2(g)$-enriched $La_2CuO_{4.032}$ superconducting sample are shown in figs. 1(a) and (b), respectively. For consistency, all data reported in this paper were obtained using one crystal although others were employed throughout this study with similar results. The indicated scale factors allow a direct comparison of the mass spectrometer oxygen signals. Whereas no measurable signal above the digitized noise limit is observed in the control experiment (fig. 1(a)), numerous rapid desorption peaks are observed from the superconductor (fig. 1(b)) as the temperature is increased above 350 K. Each peak at mass 32 ($^{16}O_2^+$) was accompanied by a simultaneous mass 16 peak ($^{16}O^+$ fragment, not shown) following the cracking pattern for $O_2(g)$, confirming that the desorbing species is molecular oxygen.

The number of desorption events, their desorption temperatures, and integrated intensities were not reproducible for various fully oxygenated crystals. However, the rapid desorption kinetics were found for all oxygen-enriched crystals. Incompletely oxygenated samples did yield fewer desorption peaks and a smaller total integrated oxygen signal, showing that the total amount of oxygen desorbed is correlated with the initial amount of interstitial oxygen. Because the crystal had to be demounted from the heating coil for oxygen-enrichment after each TDMS experiment, exact duplication of the mounted position was impossible.

The characteristically asymmetric lineshape for all peaks, illustrated in fig. 2 for an isotopically labeled sample, is indicative of unusual kinetics. The full width at half maximum (FWHM) of the connected data points is typically less than 0.5 s. As illustrated in fig. 2, the leading edge almost always consists of only one point at the maximum signal level, placing

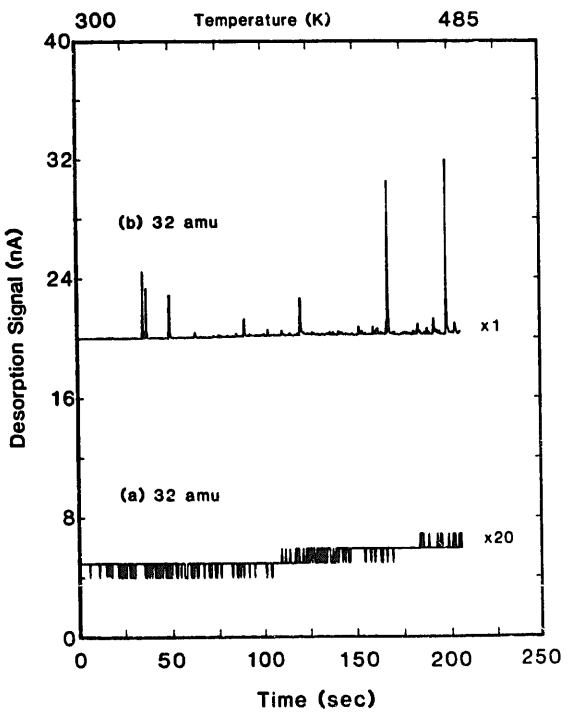

Fig. 1. Mass 32 TDMS data for (a) the insulating $La_2CuO_{4.00}$ material, and (b) the same sample after $^{16}O_2(g)$ enrichment to make a superconductor. The spectra are offset vertically for clarity and multiplicative scales are indicated to compare ion currents directly.

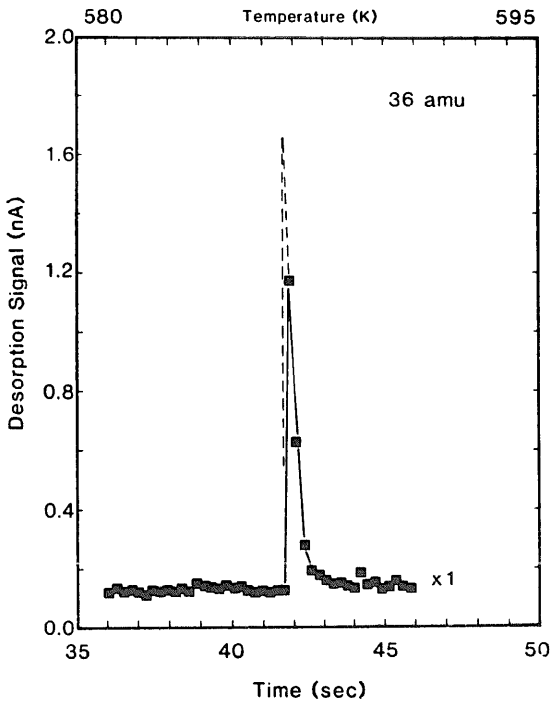

Fig. 2. An expanded mass 36 TDMS peak for $^{18}O_2(g)$ enriched $La_2CuO_{4.032}$. The data points indicated by squares are connected by solid line segments for peak integration. Dashed lines indicate an alternate peak profile for rise times below 0.2 s.

an upper limit of ~0.2 s on the actual rise time. The dashed line extrapolation suggests an alternate peak shape with a shorter rise time that is also consistent with the data points. Regardless of the interpolation chosen, the desorption event occurs over a time scale corresponding to a temperature change of less than 1 K.

The steep low-temperature side of every TDMS peak and overall asymmetric lineshape cannot be due to inhomogeneous sample heating as both the low and high temperature edges would then be broadened. In general, all peaks share a common line-shape when the peak maxima are normalized, suggesting that the pumping speed of the high-vacuum chamber determines the high temperature line-shape and resultant peak FWHM. In order for the oxygen partial pressure change, $dP(O_2)/dT$, measured by the mass spectrometer to be proportional to the oxygen desorption *rate* from the crystal, $d\Theta/dT$, the vacuum pumping speed must be large relative to the desorption rate [13,14]. These data show that this requirement is *not* met under the present conditions. Hence the intrinsic peak shape must be considerably more narrow than that shown in fig. 2, and the high-temperature side to the TDMS peak results from the slow (~1 s) vacuum recovery from the rapid burst.

Unlike the ceramic samples used in initial studies [4,5], prolonged annealing (~30 min) at a single temperature above the onset of desorption (>350 K) did not lead to continuous oxygen bursts and failed to deplete the crystals of oxygen, as demonstrated by subsequent oxygen bursts when the temperature was raised further. Also, a second temperature ramp to the same maximum temperature resulted in no additional bursts. These two results show that the desorption event is not a diffusion-limited process and that each oxygen burst is correlated with an activated process in a microcrystallite.

3.2. Oxygen exchange

Using $^{18}O_2(g)$ high-pressure enrichment and TDMS, we are able to investigate whether the dissociative incorporation of interstitial oxygen required by both the Jorgensen [8] and Chaillout [9] models involves the lattice oxygen ions, which would lead to isotopic scrambling in the TDMS data. The same crystal used for several previous TDMS experiments was isotopically enriched for 36 h at 860 K. Because of the limited quantities of $^{18}O_2(g)$ available, cryopumping into a special low volume pressure vessel was necessary for the isotopic oxygen enrichment procedure. The pressure achieved during isotopic enrichment was estimated to be 2.0 ± 0.5 kbar based upon the measured T_c and assuming a negligible isotope effect.

Typical data for a TDMS experiment are shown in fig. 3 along with scale factors for the vertically displaced spectra to allow direct comparison of the signal intensities. The experiment was performed in two temperature segments, heating at a rate of 1 K s^{-1}. Major coincident desorption peaks are identified by capital letters. If the interstitial oxygen is incorporated molecularly, only isotopically labelled $^{18}O_2(g)$ should be observed in the TDMS experiment. Likewise, if the interstitial oxygen dissociates upon enrichment, diffuses without exchanging with lattice $(^{16}O)^{2-}$ ions, and recombines when later heated, then only $^{18}O_2(g)$ should be desorbed. Some surface defects could lead to minor isotopic exchange and small $^{16}O^{18}O(g)$ TDMS peaks. Peaks at mass 32, indicative of $^{16}O_2(g)$, would be even less likely, since this would require a double exchange process.

The data clearly show that significant $^{16}O^{18}O(g)$ and $^{16}O_2(g)$ are desorbed from the crystal at all temperatures, excluding the possibility of molecular incorporation suggested in early work [4,5]. An examination of the coincident peaks in fig. 3 reveals that the mass 36 and mass 32 peaks are usually accompanied by a weak peak at mass 34; however, coincident peaks at all three masses are rare. This systematic correlation suggests that a part of the mass 34 signal is due to isotopic mixing in the mass spectrometer ionizer or on the vacuum chamber walls.

The second important observation from the data of fig. 3 is that the isotopic *distribution* of the desorbing oxygen gas changes at higher temperatures. Whereas the major product is $^{18}O_2(g)$ below 500 K, above it is $^{16}O_2(g)$. This temperature-dependent isotopic distribution provides insights into the mechanism of oxygen doping. The simplest explanation for the isotopic distribution change at high desorption temperatures would be that the $^{18}O_2(g)$ did not penetrate deeply into the $La_2CuO_{4+\delta}$ crystal and the $^{16}O_2(g)$ desorption is from the previous high-pressure enrichment. This can be ruled out since deple-

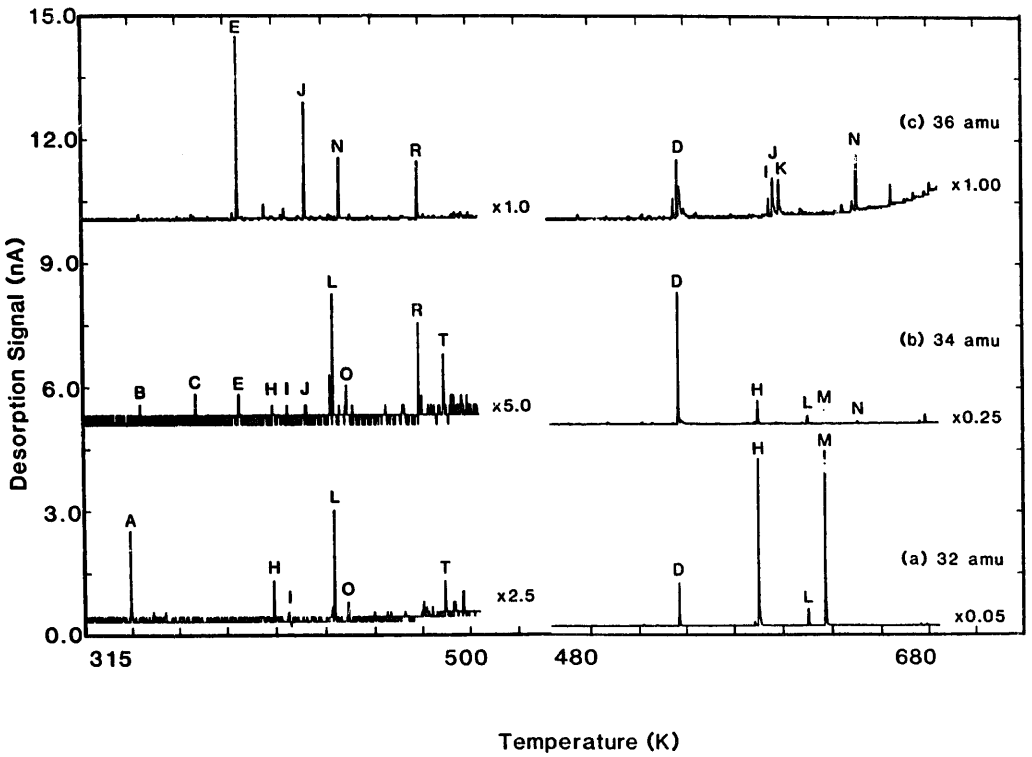

Fig. 3. Multiplexed TDMS data for 315 K < T < 680 K from a superconducting sample enriched with $^{18}O_2(g)$ for 36 h. Scale factors for the absolute signal levels of the vertically displaced spectra are shown for (a) mass 32, (b) mass 34 and (c) mass 36.

tion of the interstitial ^{16}O was confirmed by weight loss measurements and lack of superconductivity prior to the isotopic enrichment.

Instead, these results are indicative of isotopic exchange leading to a mixture of interstitial ^{16}O and ^{18}O atoms. If the $O_2(g)$ TDMS peaks at high temperatures originate from deeper within the crystal, then we can conclude that isotopic exchange must be occurring during high-pressure enrichment and not simply during the TDMS experiment. Note in fig. 3 that the low temperature TDMS peaks are mostly $^{18}O_2(g)$, meaning that lattice ^{16}O ions replaced by ^{18}O have been purged from the near-surface regions of the crystal. Conversely, the high-temperature TDMS peaks are overwhelmingly $^{16}O_2(g)$; the exchanged lattice ions were not effectively purged from the lattice during the $^{18}O_2(g)$ enrichment process.

The above interpretation has two consequences: first, a longer duration isotopic enrichment with $^{18}O_2(g)$ should purge the exchanged ^{16}O from the crystal and lead to a less temperature-dependent isotopic distribution; second, the ^{18}O which has exchanged with lattice ion sites should be evident as a net weight gain even after all of the interstitial oxygen is desorbed by the TDMS experiment.

These consequences were tested by an additional 100 h of 98% pure $^{18}O_2(g)$ enrichment. The parameters in the TDMS experiment were modified slightly to permit more rapid sampling of the three mass channels of interest; as a consequence, the 300–680 K desorption experiment was conducted in three temperature intervals, shown in fig. 4, rather than in two segments. As expected, mass 36 signal are dominant below 445 K. In contrast to fig. 3, however, above 445 K all mass fragments are observed with comparable peak intensities, confirming the first expectation, listed above.

The weight gain expected as a result of isotopic exchange is shown in fig. 5 which summarizes a series of TDMS experiments for one crystal. Solid and open circles represent the crystal weight before and after each TDMS experiment, respectively. For this crystal, three enrichments with $^{16}O_2(g)$ were followed by the 36 h and 100 h $^{18}O_2(g)$ enrichments, and, finally, one with $^{16}O_2(g)$. As noted previously, the difference in weight before and after each TDMS ex-

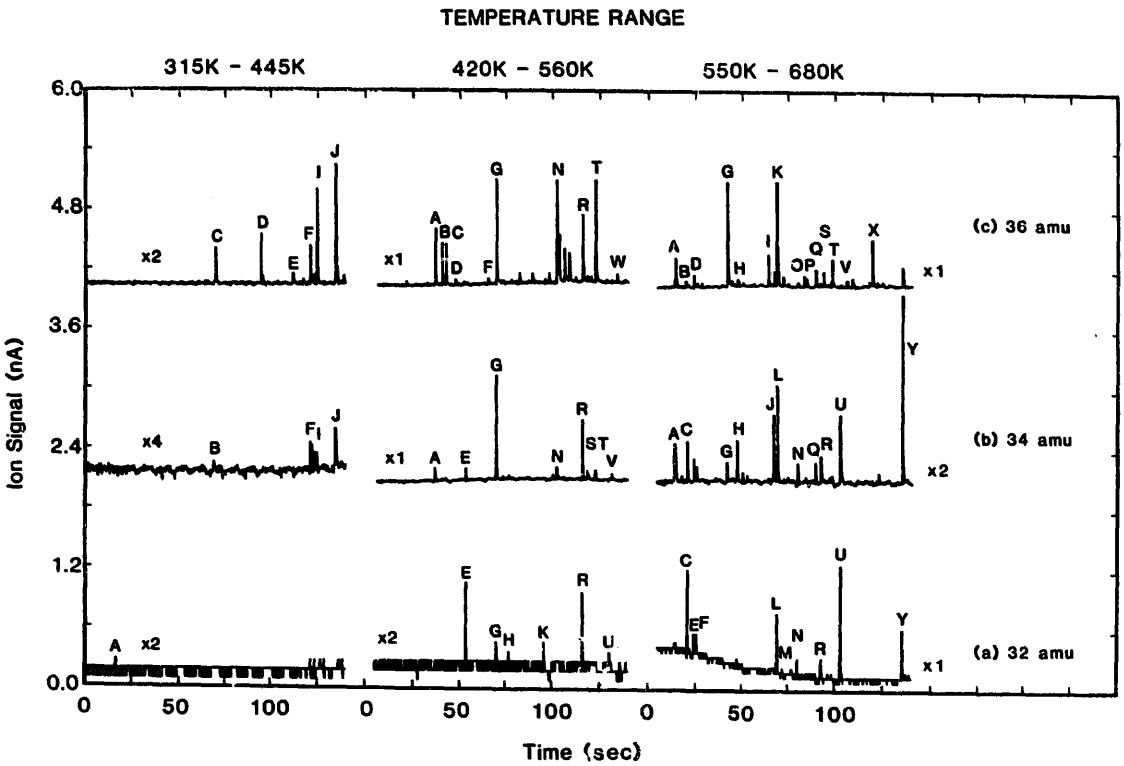

Fig. 4. TDMS data for 315 K < T < 680 K from the same sample after additional enrichment with $^{18}O_2(g)$ for 100 h. Vertically displaced spectra are shown with scale factors for the absolute signal levels for (a) mass 32, (b) mass 34 and (c) mass 36.

periment – corresponding to only the interstitial oxygen lost by thermal desorption – is within the experimental error regardless of the isotopic identity. However, an large *absolute* weight gain is found after each of the two $^{18}O_2(g)$ enrichment/desorption cycles, corresponding to a net increase in mass even after desorbing the interstitial oxygen. This can *only* be due to a substantial substitution of lattice ^{16}O ions with ^{18}O ions during high pressure enrichment. Since the lattice ions are unaffected by the TDMS heating to 680 K, the resultant weight gain is a measure of the amount of oxygen exchanged. Furthermore, we note that the weight gain after the 100 h enrichment is less than that after the first 36 h enrichment. Extrapolation of this trend indicates that unreasonably long times, or much higher $^{18}O_2(g)$ pressures, would be required to establish the maximum isotopic exchange possible in this crystal.

As a final test of the isotopic exchange, the crystal was re-enriched using $^{16}O_2(g)$. In this case, the exchange mechanism will replace the lattice sites with ^{16}O ions, lowering the crystal weight to nearly the original value. The last solid circle in fig. 5 shows that most of the ^{18}O was purged from the lattice and interstitial sites after this one step.

4. Discussion

Thermal desorption mass spectroscopy is a well-developed technique to measure desorption kinetics and energetics from a solid surface [13,14], and thereby address the mechanism of the desorption process. For $O_2(g)$ desorption from oxygen-enriched $La_2CuO_{4.032}$, the process would be expected to be rate limited by diffusion from the bulk to the surface ($O(bulk) \rightarrow O(ads)$), recombination of atomic oxygen ($2\,O(ads) \rightarrow O_2(ads)$), or molecular desorption [$O_2(ads) \rightarrow O_2(g)$]. As a result, the desorption kinetics would be expected to be first or second order, depending upon which step is actually rate limiting.

The TDMS peak shape and multiple events over a range of temperatures are inconsistent with these

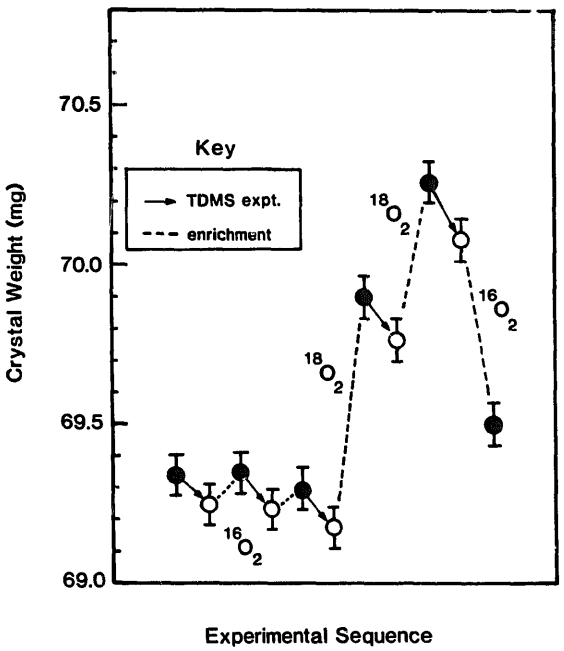

Fig. 5. Summary of weight measurements for the La_2CuO_4 crystal used for all TDMS data shown.

kinetic mechanisms and could not be due to inhomogeneous heating. For desorption from a solid *surface* alone, a temperature gradient across the surface simply broadens the TDMS peak as various areas contribute a delayed desorption signal with respect to the temperature measured at the thermocouple junction. The transient line-shape shown in fig. 2 is distinctly different from the functional forms characteristic of first-order or second-order desorption processes [14]. Diffusion-limited desorption should yield oxygen TDMS signals over relatively long time scales due to the slow heating rate used in this experiment and would be manifested by broad desorption peaks.

We propose a simple explanation for the rapid oxygen bursts. From the diffraction studies by others, it is known that the bulk undergoes phase transitions which involve interstitial oxygen segregation. As the temperature is increased, interstitial oxygen segregation within the crystal can induce lattice stresses as each domain attempts to revert to the $LaCuO_{4.00}$ tetragonal crystal structure ($T > 280$ K) but is constrained by the surrounding bulk lattice. This stress is ultimately relieved by lattice fracture during the TDMS experiment, releasing the trapped oxygen from the sample in bursts as micro-cracks are formed. Stress-induced crystal fracture is not uncommon for crystalline phase transformations that involve lattice expansions and contractions [15], and would be exacerbated by both the twinned nature of the crystal and inhomogeneous sample heating. Within this model, the range of temperatures over which the bursts are observed reflects the activation energies required to fracture the lattice in different places.

One variation on the proposed model is that voids exist within the bulk , to which the interstitial oxygen diffuses, forming trapped gas bubbles which mechanically break the crystal when annealed to >400 K. Although we cannot preclude this possibility, it is not necessary to explain the data. The oxygen trapped at internal surfaces such as grain boundaries need not have recombined to lead to fracturing [15].

The isotopic data and weight measurements show that isotopic exchange occurs during high-pressure oxygen enrichment. The crystal weight data shown in fig. 5 can be used to determine that approximately 50% of the total lattice oxygen has exchanged with ^{18}O after a total of 136 h of treatment. It is not known whether more robust enrichment conditions would increase the fraction of lattice ions exchanged. Certainly a concentration gradient in favor of ^{18}O is expected near the surface of the crystal as the exchanged ^{16}O is more likely to have diffused out of the bulk. However, we know that oxygen diffusion cannot be facile, otherwise complete equilibrium would be established and the mobile ^{16}O atoms would be diluted to less than 2% of the oxygen desorption signal.

5. Conclusions

The interstitial oxygen in superconducting $La_2CuO_{4+\delta}$ is shown to thermally desorb in transients of FWHM ≈ 0.2 s. Desorption is not bulk diffusion limited, nor can the desorption rate be modeled as simple first or second order kinetics of Arrhenius form. Instead, an explanation is proposed in which segregation of interstitial oxygen leads to internal lattice fracture, thereby releasing trapped $O_2(g)$. Isotopic labeling experiments show that oxygen diffusion proceeds via exchange with lattice oxygen ions, with up to 50% of the lattice sites having

exchanged under the present conditions. the activation energy for this exchange is less than that for oxygen diffusion. These results exclude structural models for $La_2CuO_{4+\delta}$ involving interstitial molecules.

Acknowledgements

This work is supported by the United States Department of Energy, Office of Basic Energy Sciences, Division of Material Sciences, under contract DE-AC04-76DP00789 with Sandia National Laboratories. Discussions with Edwin Beauchamp and Bruno Morosin are gratefully acknowledged.

References

[1] J.E. Schirber, E.L. Venturini, B. Morosin, J.F. Kwak, D.S. Ginley and R.J. Baughman, in: High-Temperature Superconductors, Boston, MA, 1987 eds. M.B. Brodsky, R.C. Dynes, K. Kitazawa and H.L. Tuller, Mater. Res. Soc. Proc., vol. 99 (Mater. Res. Soc., Pittsburgh, PA, 1988) p. 479.

[2] S.-W. Cheong, J.D. Thompson and Z. Fisk, Physica C 158 (1989) 109.

[3] J. Beille, B. Chevalier, G. Demazeau, F. Deslandes, J. Etourneau, O. Laborde, C Michel, P. Lejay, J. Provost, B. Raveau, A. Sulpice, J.L. Tholence and R. Tournier, Physica B 146 (1987) 307.

[4] J.E. Schirber, B. Morosin, R.M. Merrill, P.F. Hlava, E.L. Venturini, J.F. Kwak, P.J. Nigrey, R.J. Baughman and D.S. Ginley, Physica C 152 (1988) 121.

[5] J.W. Rogers Jr., N.D. Shinn, J.E. Schirber, E.L. Venturini, D.S. Ginley and B. Morosin, Phys. Rev. B 38 (1988) 5021.

[6] C. Chaillout, S.-W. Cheong, Z. Fisk, M.S. Lehmann, M. Marezio, B. Morosin and J.E. Schirber, Physica C 158 (1989) 183.

[7] (a) J. Zhou, S. Sinha and J.B. Goodenough, Phys. Rev. B 39 (1989) 12331;
(b) J.W. Rogers Jr., N.D. Shinn, J.E. Schirber, E.L. Venturini, D.S. Ginley, and B. Morosin, Phys. Rev. B 39 (1989) 12334.

[8] J.D. Jorgensen, B. Dabrowski, Shiyou, D.R. Richards and F.G. Hinks, Phys. Rev. B 40 (1989) 2187.

[9] (a) C. Chaillout, J. Chenavas, S.-W. Cheong, Z. Fisk, M.S. Lehmann, M. Marezio, B. Morosin and J.E. Schirber, Physica C 162–164 (1989) 57;
(b) C. Chaillout, J. Chenavas, S.-W. Cheong, Z. Fisk, M. Marezio, B. Morosin and J.E. Schirber, Physica C 170 (1990) 87.

[10] J.D. Jorgensen, B. Dabrowski, S. Pei, D.G. Hinks, L. Soderholm, B. Morosin, J.E. Schirber, E.L. Venturini and D.S. Ginley, Phys. Rev. B 38 (1988) 11337.

[11] P. Zolliker, D.E. Cox, J.B. Parise, E.M. McCarron III and W.E. Farneth, to be published.

[12] M.F. Hundley, J.D. Thompson, S.-W. Cheong, Z. Fisk and J.E. Schirber, Phys. Rev. B 41 (1990) 4062.

[13] P.A. Redhead, Trans. Far. Soc. 57 (1961) 641;
ibid., Vacuum 12 (1962) 203.

[14] D.A. King, Surf. Sci. 47 (1975) 384.

[15] R.W. Rice and R.C. Pohanka, J. Am. Ceram. Soc. 62 (1979) 559.